A Case Study Comparing the Lossy Wave Equation to the Continuity Equation in Modeling Late-Time Fields Associated with Lightning*

Michael E. Baginski A. Scottedward Hodel

Abstract

An investigation is presented into lightning-related transient electric fields and conduction current densities due to the redistribution of charge by the return stroke (late-time effects). A qualitative comparison is made between the late-time vertical electrical field magnitudes predicted by two solutions via the continuity equation/Poisson's equation and the continuity equation in conjunction with the lossy wave equation. The differences between these results indicate that the magnetic energy density created by a lightning discharge generally provides relevant changes in the resulting electrical field waveforms as radial and vertical distances increase from the lightning discharge. That is, the accuracy of the conservative field assumption $\nabla \times E = 0$ decreases with the distance from the point of excitation to the point of observation of the electric field for the study conducted. This observation suggests the use of the lossy full wave equation, when computationally feasible, for the prediction of late-time electric field behavior. This study addresses trends in the general behavior of the two solutions over region $0 \leq r \leq 30$ km and $30 \leq z \leq 50$ km.

1 Introduction

The purpose of this research is to examine the necessity of using both Ampere's current law and Faraday's law on induction as opposed to using the quasi-static solution to describe the late-time field recovery of electromagnetic transients associated with lightning. This has been a major area of controversy for several decades [1], [2], [3] due to the fact that solutions based on quasi-static analysis are far simpler to solve numerically and to formulate than solutions based on the lossy wave equation. In the following, a brief overview of some of the previous research and the true nature of the problem to be discussed is presented.

Late-time electromagnetic fields stem from the non-propagating portion of the electromagnetic transient from lighting and are therefore associated with the electrostatic and magnetostatic energy created when lightning occurs. Since a multitude of approximations are required in the modeling of the late-time effects of the lightning event, the digital simulations presented in the following sections employed commonly accepted charge distributions conductivity profiles, and general atmospheric parameters [4], [5]. It is hoped that this research will be of value not only to atmospheric scientists but also those studying EMP, HEMP, corona discharges, etc.

In this work, a finite element code was used to compute the vertical electric fields in the middle atmosphere via (1) the continuity equation

$$\nabla \cdot J + \frac{\partial \rho}{\partial t} = 0$$

and Poisson's equation

$$\nabla^2 \phi = -\frac{\rho}{\epsilon_0},$$

and (2) the complete set of Maxwell's equations

$$\begin{aligned} \nabla \times E &= -\mu_0 \frac{\partial H}{\partial t} \\ \nabla \times H &= \sigma E + \epsilon_0 \frac{\partial E}{\partial t} + \text{additional sources of charge movement.} \end{aligned}$$

Both sets of equations used identical atmospheric parameters. The respective vertical electric field waveforms were then compared with waveforms over a wide range of values of radial distance r and altitude z. A detailed analysis of the waveforms generated by the two different numerical solutions was performed

*The authors are with the Auburn University Department of Electrical Engineering, 200 Broun Hall, Auburn AL 36849

by comparing the mean squared error difference between the solutions. The results showed that there is a radial and vertical position where the electric field signatures begin to deviate significantly from one another. It is the view of the authors that this would be the logical region that would mandate the use of the complete set of the Maxwell equations. It should be emphasized that the results presented herein are only for a specific set of atmospheric conditions and, thus, may show sensitivity to several atmospheric parameters.

2 Historical Perspective

Since the 1950's several electrical models describing the interaction of thunderstorms with the atmosphere have been published. Holzer and Saxon [6] have assumed concentrated charges in a dipole configuration with spatially varying conductivities to obtain temporally invariant field patterns in the lower atmosphere and ionosphere. The lightning return stroke, however, generates transients in the electric field pattern known as "field changes" [7]. Early workers attributed this temporal recovery to recharging within the thundercloud. Tamura [8] is credited as the first to note that the surrounding atmosphere is also involved. He defined solutions based on the conservative field assumption (i.e., $\nabla \times E = 0$) that depend on the conductivity at the point of observation. Kasmir [9] constructed the first dynamic model of the thundercloud system using resistors, a capacitor, and a spark gap. His model connected a current generator, a capacitor, and a resistor in parallel to model the cloud ionospheric connections with the path to earth replaced by a resistor. More dynamic models began to follow. Anderson and Freier [10] incorporated dynamic changes in the dipole structure with spatially varying conductivities. However, they only include the quasi-static relaxation in their model instead of solving the total set of Maxwell's equations. Additional solutions were developed based on the "monopole" model of Wilson [11], Illingworth [12], Park and Dejnakarintra [13], Greifinger and Greifinger [14], Holzworth and Chiu [5], Baginski *et al* [15], and Driscoll *et al* [16]. The transient lightning event was investigated recently by Hoole and Hoole [17] using a finite element code. Discussion on guided waves in lightning plasma channels is presented in [18].

3 Thunderstorm Modeling

3.1 Charging Mechanisms

The most difficult phenomenon to explain in thunderstorm research has been the process involved in cloud electrification. The difficulty is twofold: Firstly, there exist a large number of possible mechanisms responsible for charge separation and current generation; further, it is usually impossible to isolate such mechanisms and test each for its relative effect. Regardless of the mechanisms, what is known is that a thunderstorm is sustained by a charge separation which can be approximated by net positive and negative charge centers. The height of the charge centers is somewhat affected by seasonal changes and the geographic location. Typical heights of 10 km for the upper charge center and 6 km for the lower charge center are widely found in the literature and have been selected for this research [19]

The magnitudes and profiles of the charge centers and currents vary significantly from storm to storm. Kasmir [9], for instance, has measured values ranging from 20 C up to 1000 C for thundercloud charges and cloud electrification currents from less than 0.1 A to 10 A. Lightning return stroke currents are reported to have an even larger range of values [7]. The existence of such large variations complicates selection of the currents and the charge deposition profile. After a review of the relevant literature [20], [14], a choice of the forcing current and profile of charge deposition was made. The selection was based upon widely used current and charge profiles. The charge perturbation used was developed based on Sunde's [4], [20] lightning return stroke current model.

Sunde's [20] lightning return stroke model is selected for this research primarily because of its extensive commercial and military use in work requiring an analytic formulation of the lightning return stroke current. This model was developed based on the statistics of a very large number of measurements during lightning events. Sunde's model is relatively simple compared to some [7], but includes the fundamental attributes necessary to predict "average" electromagnetic field behavior [20]. The charge generation (in units of A or C/s) may be expressed in terms of this lightning return stroke current temporally as follows:

$$G_s = \frac{dQ(t)}{dt} = i(t) = I_0 \left(e^{-at} - e^{-bt}\right) \qquad (3.1)$$

where $i(t)$ = the lightning return stroke current from

Sunde's modified model, $a = 10^4\ s^{-1}$, $b = 0.1 \times 10^3\ s^{-1}$, and I_0 is proportional to the amount of charge displaced during the return stroke.

It is well known that the deposition of charge from the return stroke current is primarily responsible for the charge perturbation [21]. The deposition rate of charge due to the the lightning return stroke current is proportional to the time derivative of the charge perturbation [19]. Therefore, the total charge deposited at time t may be expressed as the integral of the lightning return stroke current in time, given by

$$Q(t) = \int i(t)dt \tag{3.2}$$

where $i(t)$ is the lightning return stroke current and $Q(t)$ is the total displaced charge of the return stroke.

Consider equation (3.1). The term e^{-bt} describes the rise time of the charge generation inducing the perturbation, i.e., how rapidly the maximum return stroke current, but not charged deposited, is attained. Since the amount of charge exchanged during a return stroke is related to its time integration, omission of the term e^{-bt} causes no appreciable change (for time greater than 5×10^{-6} s) in the amount of charge displaced, and therefore, no appreciable change in the simulated electrodynamic response. The spatial and temporal structure of the deposited charge G_s is given by a modified spherical Gaussian profile:

$$G_s = (2\pi\lambda)^{-1.5}\exp\left(-\frac{r^2+(z-z')^2}{2\lambda}\right) \times \left(\frac{e^{-t/\tau_1}}{\tau_1}\right) \tag{3.3}$$

where

τ_1 = 10^{-3} s is the decay time of the force charge event

λ = 4×10^6 m^2 is the effective variance

z' = the altitude of the charge perturbation.

The spatial distribution of the charge perturbation does not noticeably affect electric field signatures far from its interior [4]. This condition exists for our model (electrical fields of interest in the present study are at least 20 km from the charge perturbation) which allows a certain degree of freedom in the specification of the distribution. Also, since virtually no published data is available describing the spatial structure of the deposition of the charge from the lightning return stroke current [22], the selection is even more arbitrary. Further, the modified Gaussian distribution is used in the modeling of many man-made and naturally occurring forced charge events [4] which justifies our choice for this model.

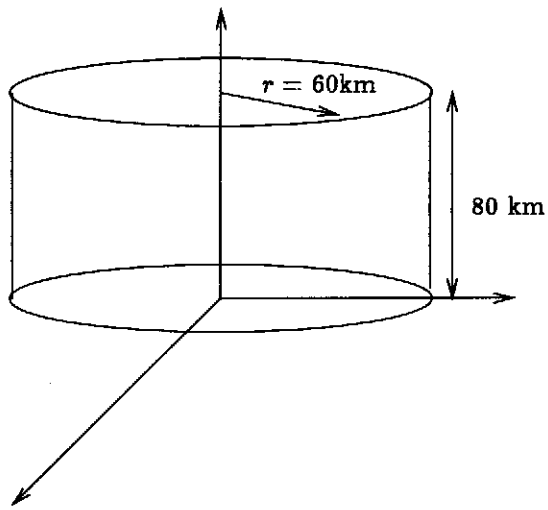

Figure 1: Region of simulation

Geometry of the Region: Before describing the geometry, consider again the phenomenon of interest: charge perturbations, located at altitudes no greater than approximately 10 km, induce electric fields throughout the atmosphere, but only those fields induced within the middle atmosphere are to be simulated. Thus,

1. If not obviously constrained, the geometrical limits of the model will approximate the entire atmosphere's electrical effect on the regions where the simulations take place.

2. The boundary conditions of the region will be electrically equivalent to those of the atmosphere.

The region selected (Figure 1) is contained within a perfectly conducting right circular cylinder with a radius of 60 km and height of 80 km. A discussion of how each of the boundaries was arrived at follows:

Lower Plate: The earth's surface is electrically modeled as a perfect conductor. This assumption is based on the very large difference that exists between the

earth's conductivity and adjacent atmosphere's conductivity. Typical values of .001 to 0.01 mhos/m [23] are given for the earth's conductivity, while 10^{-13} to 10^{-14} mhos/m is the usual range of the adjacent atmosphere's conductivity. This difference of more than 11 orders of magnitude makes the earth appear (electrically) as a perfect conductor.

Upper Plate: The selection of 80 km for the height of the upper boundary was a necessary consequence since the atmospheric conductivity structure is complicated by the Hall and Pederson components above an altitude of approximately 70 km [24]. The tensor conductivity components result when the mean free path and velocities of the charge carriers are sufficient to allow their trajectories to be altered by the effect of the earth's magnetic field [25]. In the present model tensor quantities have been excluded to keep the algorithm simple without adversely affecting numerical accuracy. Further, in past studies [3], [2] an altitude limit is set in the vicinity of 70 km. Dejnakarintra and Park [2] note that this level is an appropriate choice since the conductivity becomes anisotropic at this altitude.

For this study, the 80 km altitude was selected based on the following considerations:

1. The relative magnitude of the Hall and Pederson tensor conductivity components is approximately proportional to the additional distance in altitude (beyond 70 km) considered, i.e., the difference in components is proportional to $(z-70)$. The maximum value of either of these components with respect to the parallel σ conductivity's magnitude (for the range of altitudes considered) is less than 10 percent [24].

2. The middle and upper atmospheric electric fields resulting from lightning (with the exception of the propagating component) are approximately vertically oriented [24], i.e., the horizontal component is negligible.

3. The off-diagonal tensor components of the high-altitude conductivity only interact with electric fields that are not aligned with the earth's magnetic field [24]. Since the earth's magnetic field, with the exception of the equatorial regions, is primarily vertically aligned [21], the influence of both the Pederson and Hall components on the lightning-induced vertical electric fields will be, to first order, negligible. The inclusion of these components would tend to prolong the simulated atmospheric transient response at altitudes of 70 km and above. Since this investigation focuses on altitudes less 50 km the impact of these terms on our results would be insignificant.

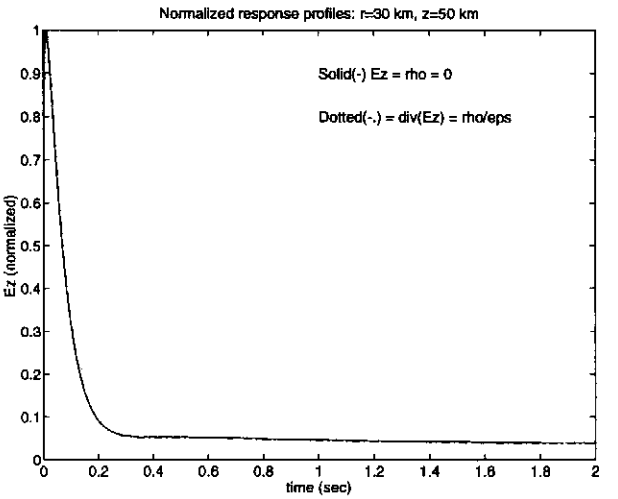

Figure 2: Effect of 80 km upper plate in vertical E-field computation

An obvious concern is the influence this 80 km altitude limit may have on the simulations. A previous study [3] used simulations based on the full wave equation to determine the maximum error in the vertical electric field in the region of interest in the present study. The results showed that the maximum electric field error induced by the 80 km ceiling occurs at $z = 50$ km and produced a relative error of less than 1%. To investigate the maximum possible error in the electric field due to this assumption (assuming an electrically passive atmosphere), two further sets of simulations were conducted with the 80 km upper plate electrically described by: 1) The vertical electric field and charge density are set to zero ($E_z = \rho = 0$). 2) The divergence of the electric field is set to the value of the charge density divided by the permittivity of free space ($\nabla \cdot E = \rho/\epsilon$). These simulations indicate a maximum error at radial distance $r = 30$ km and altitude $z = 50$ km. A representative plot of respective vertical waveforms is shown in Figure 2. Use of the conservative field assumption reduces the associated error even further. The change in the two boundary conditions provided above pro-

vides a worst-case error analysis. In all simulations, comparison of results showed little if any difference for the time frames of interest (0-2 s).

The probable reason for this behavior is that in general, for lightning-induced transients, the electric properties of the atmosphere below the point of observation of the field rather than above it, govern the transient's response [26]. This may be explained by simply considering the fact that, in general, the conductivity rapidly increases with altitude (i.e. resistivity decreasing), and therefore its influence (restrictive effect) on the total global charge movement decreases. Hence, it seems reasonable to assume the middle atmosphere's simulated response to low-altitude charge perturbations is governed by the adjacent and lower altitude conductivity values.

Outer Cylindrical Surface: The lateral boundary had no distance constraint and could have been extended indefinitely. However, there exists a tradeoff between resolution (both temporal and spatial), and computational resources: reduction in the model dimensions yields improved accuracy in numerical solution of the differential equations. Therefore, the errors resulting from the adoption of finite boundaries for the model must be weighed against those resulting from degrading the numerical resolution of the code by involving too large a volume.

The simulations were found to be insensitive to increases in the radial limit beyond 50 km. No visible difference could be detected in the response using either the 50 km or 60 km radial boundaries when plotted together; see Figure 3. Therefore, selecting the 60 km radial limit is a measure to provide additional confidence in the simulations.

Axis of Symmetry: Since $r = 0$ defines an axis of symmetry and since there are no discontinuities in the charge distribution, the derivatives of the vertical electric field ($\partial E_z/\partial r$) with respect to radial distance reduces to zero on this axis.

The differential forms of the four boundary conditions are summarized as follows:

1. At the z-axis, $\partial E_z/\partial r = 0$
2. at the upper and lower boundaries $E_r = 0$
3. at the outer radial boundary $E_z = 0$

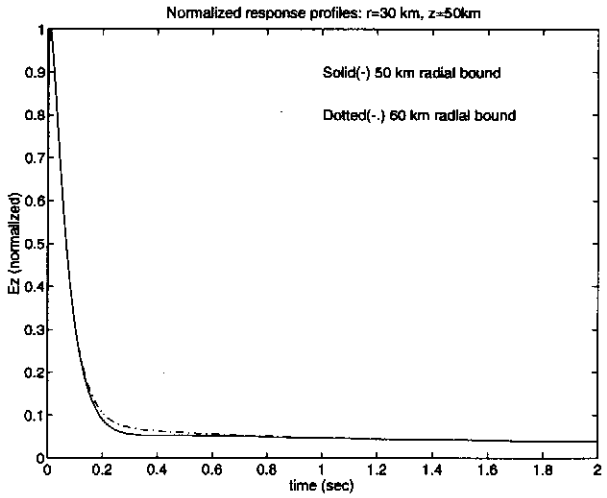

Figure 3: Effects of changes in radial limits on E-field computations.

Maxwell's Equations: To those familiar with classical electromagnetism, the analysis of the post-stroke atmospheric response may seem rather simple at first. A charge imbalance induced in a conducting region would be expected to decay exponentially with time at a rate determined by the local relaxation time of the region [25]. The corresponding electric fields, being proportional to the overall charge distribution, should decay in a like manner. When electric field measurements obtained from parachute-borne payloads [27] are considered, however, a significant deviation from the exponential decay is at times observed. In some cases a gradual peaking is observed hundreds of ms after the return stroke has ceased. This behavior suggests, at least for some circumstances, that a more complicated description is required and that a careful analysis of the governing equations should be undertaken.

Beginning with Maxwell's equations, a single equation is derived where the electric field is dependent on the charge density only as follows:

$$\nabla \times E = -\mu \frac{\partial H}{\partial t} \tag{3.4}$$

$$\nabla \times H = J + \frac{\partial D}{\partial t} + \text{additional sources of charge movement} \tag{3.5}$$

$$\nabla \cdot D = \rho \tag{3.6}$$

$$\nabla \cdot H = 0 \tag{3.7}$$

$$J = \sigma E \quad (3.8)$$
$$D = \epsilon E \quad (3.9)$$

By taking the divergence of the $\nabla \times H$ we derive the continuity equation that will be used in the analysis of both systems of simulations:

$$0 = \sigma\rho/\epsilon + \nabla\sigma \cdot E + \frac{\partial \rho}{\partial t} + G_s \quad (3.10)$$

where $G_s = \nabla \cdot J_f$ and J_f is the source charge generator causing the perturbation.

The lossy wave equation is developed using the above equations:

$$\nabla \times \nabla \times E = -\mu\sigma\frac{\partial}{\partial t} - \mu\epsilon\frac{\partial^2 E}{\partial t^2} \quad (3.11)$$

$$\nabla\rho/\epsilon = \nabla^2 E - \mu\left(\sigma\frac{\partial E}{\partial t} + \frac{\partial J_f}{\partial t}\right) - \mu\epsilon\frac{\partial^2 E}{\partial t^2} \quad (3.12)$$

The resulting second order partial differential equation is analytically solvable for only the simplest cases. The types of solutions required for altitude-dependent conductivities are not obvious. If one wishes to pursue this problem further, assumptions must be made or numerical methods must be applied. The most common assumption used in the past (e.g., [12], [1]) is to define the electric field as the gradient of the electric potential ($E = -\nabla\phi$), the conservative field equation. The mathematical consequence of this, if strictly enforced, is to constrain the electric field to decay exponentially in time. This can be shown as follows: $E = -\nabla\phi$ yields the vector identity

$$\nabla \times E = \nabla \times (-\nabla\phi) = 0. \quad (3.13)$$

Equation (3.4) and equation (3.13) imply that

$$-\mu\frac{\partial H}{\partial t} = \nabla \times (-\nabla\phi) = 0$$

i.e., H is time invariant. Since the H field in this case is time invariant, the E field is necessarily time-invariant as well for the study conducted. The general solution for the electric field is given by

$$E(r,z,t) = E_0(r,z)\exp(-t/\tau(r,z)) + E_1(r,z) \quad (3.14)$$

where $\tau(r,z) = \epsilon/\sigma(r,z)$.

This type of solution has a definite range of validity. However, for the general case, a computer solution of the above equation, not limited by the conservative field assumption, would provide more information about the true time dependent shape of the electric field. The final equation required for both simulations is the continuity equation. This is derived by taking the divergence of equation (3.14).

Critical comments on the Full Wave Equation

There are several questions that need to be addressed prior to continuing this discussion in regard to the use of the lossy full wave equation. The first is the usual spatial/temporal requirement that generally must not be violated and depends on the number of dimensions. (That is,

$$c\Delta t \leq h/\sqrt{n},$$

where h is the spatial step and n is the number of dimensions). However one can use the theory put forth by Courant and Hilbert [28] that shows that the above inequality can be modified for certain circumstances, especially when the region analyzed is lossy (i.e., σ is non-zero). (Kunz and Luebers [29] have presented a similar theory for the time-domain finite difference method.) In the lossy full wave equation used in the research, the grid size and time step were reduced until no appreciable difference was observed in the results and thereby confirm their assertions.

A second point to be made is that because of the extremely high amount of loss (very low Q) of the region, the propagation delay caused by the $\mu\epsilon\partial^2 E/\partial t^2$ term is of negligible significance compared with the loss associated with either $\mu\sigma\partial E/\partial t$ (lossy full wave equation) or the continuity equation. When several preliminary computer simulations were conducted, the actual number of triangles required to achieve accurate results was found to be 520 with a final triangulation being proportional to $r^{-1/2}$ where r is the distance from the charge center. A simulation was also performed with 1000 triangles; no significant deviation was observed from results with 520 triangles. (Quadratic elements were used in all simulations in this study; the final triangulation is shown in Figure 4.) The time step was also made proportional to $t^{-0.55}$. These two deviations from the traditional stability criteria were a cause of concern in earlier related research [15]. For comparison, simulations were also performed using a uniform mesh with uniform grid spacing in space and a constant time step; no appreciable difference was observed between the

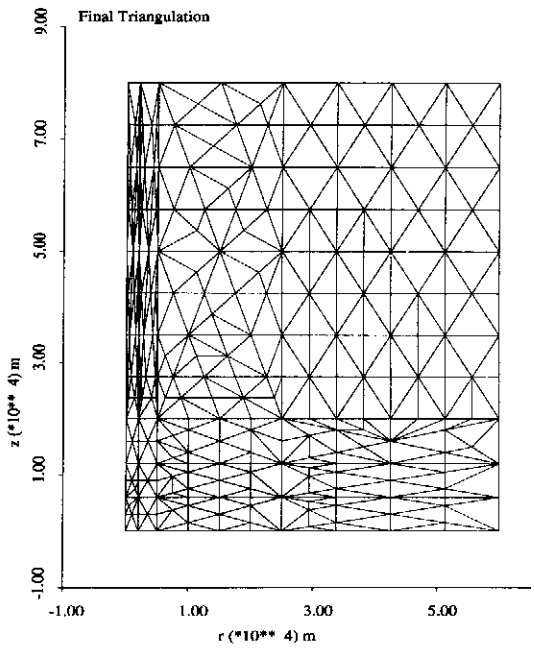

Figure 4: Triangulation used in simulations

computed solutions. The obvious benefit of the use of non-uniform mesh and varoab;e time steps is that there are enormous savings in CPU time and in-core memory. In our experiments, a single simulation involved 12-15 hours of computation on a SPARC 10 computer with the method used and probably would have required at least an order of magnitude more time if the time step and grid spacing were based on the stability criteria stated above for the time step derived from the rise time of the charge perturbation waveform.

3.2 Summary of the two equations used

The two sets of equations that are used in the comparative simulations are the following:

SET 1

$$0 = \sigma\rho/\epsilon + \nabla\sigma \cdot E + \frac{\partial \rho}{\partial t} + G_s \quad (3.15)$$

$$0 = \nabla^2\phi + \rho/\epsilon \quad (3.16)$$

SET 2

$$\nabla\rho/\epsilon = \nabla^2 E - \mu\left(\epsilon\frac{\partial E}{\partial t} + \frac{\partial J_f}{\partial t}\right) - \mu\epsilon\frac{\partial^2 E}{\partial t^2} \quad (3.17)$$

$$0 = \sigma\rho/\epsilon + \nabla\sigma \cdot E + \frac{\partial \rho}{\partial t} + G_s \quad (3.18)$$

where $G_s = \nabla \cdot J_f$.

4 Numerical Results

As stated earlier, the intent of this research was to investigate, via a finite element code based on a solution of the differential equations [30], [31] the necessity of solving the lossy full wave equation (3 equations) versus the much less computer intensive conservative field equations for charge perturbations in the middle atmosphere. The method used will now be presented. The comparison was based on the use of the mean squared error difference between the two simulations to identify the difference versus position and time. The grid used was spaced radially at points of $r = 0, 5, 10, 15, 20, 25$, and 30 km and at altitudes of $z = 30, 35, 40, 45$,and 50 km.

Let $e_\infty(r, z, t)$ denote the magnitude of the electric field at radial distance r, altitude z, and time t, under the assumption that Faraday's law of induction is omitted; i.e., when using only the continuity equation (3.15) and Poisson's equation (3.16). Similarly, let $e_c(r, z, t)$ denote the electric field when using the full wave equation (3.17) in tandem with the continuity equation (3.18). The PROTRAN program [30] was used to compute e_∞ and e_c over a range of radial distances r and altitudes z for several seconds. A sample plot comparing the computed electric fields at radial distance 20 km are shown in Figures 5–9. (In Figures 5–9 the solid line denotes the quasi-static simulation (e_∞) and the broken line denotes the solution to the lossy full wave equation (e_c).)

In order to determine quantitatively the effects of the magnetic energy density on late-time electric-field magnitude, an error signal

$$\gamma(r, z, t) = e_\infty(r, z, t) - e_c(r, z, t)$$

was computed and an RMS error was normalized against the energy in $e_\infty(r, z, t)$ by computing

$$w(r, z, t) = \left(\frac{|\gamma(r, z, t)|^2\, dt}{|e_\infty(r, z, t)|^2\, dt}\right)^{1/2}. \quad (4.1)$$

Time-varying plots of $w(r, z, t)$ vs altitude and time are shown for varying radial distances r in figures Figure 10–Figure 16.

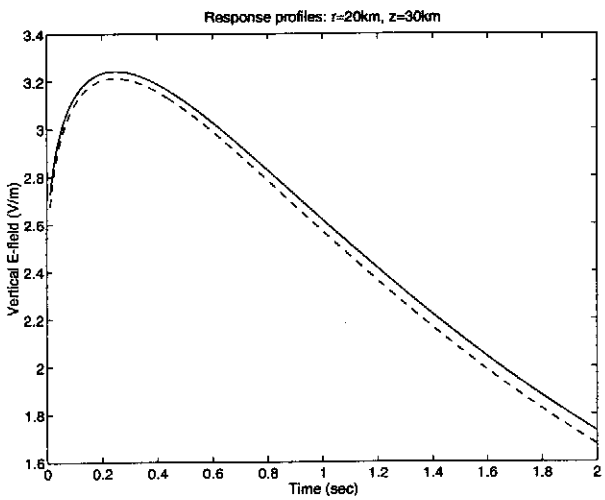

Figure 5: Electric field transient (altitude 30km)

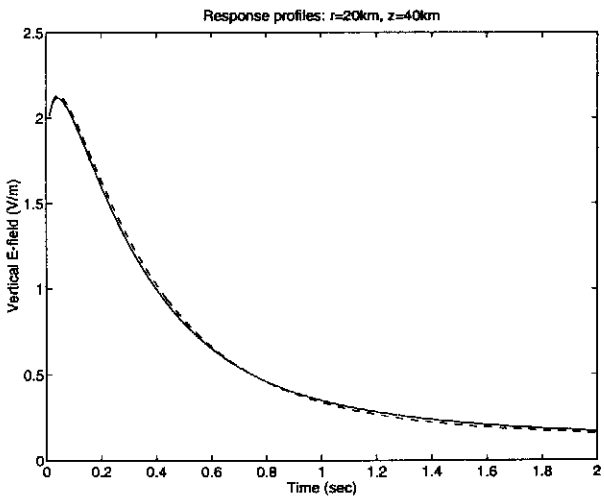

Figure 7: Electric field transient (altitude 40km)

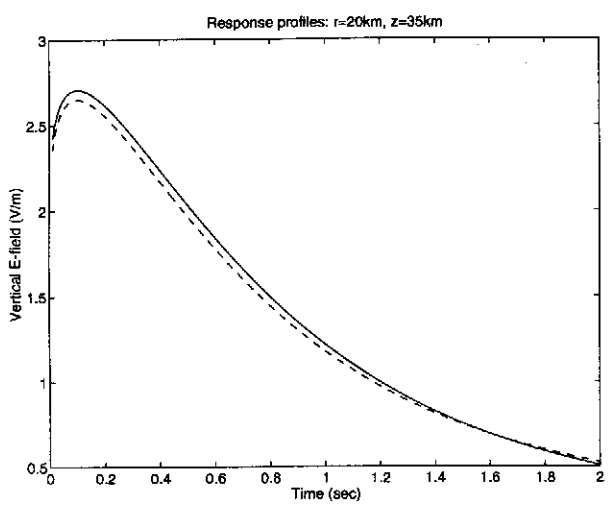

Figure 6: Electric field transient (altitude 35km)

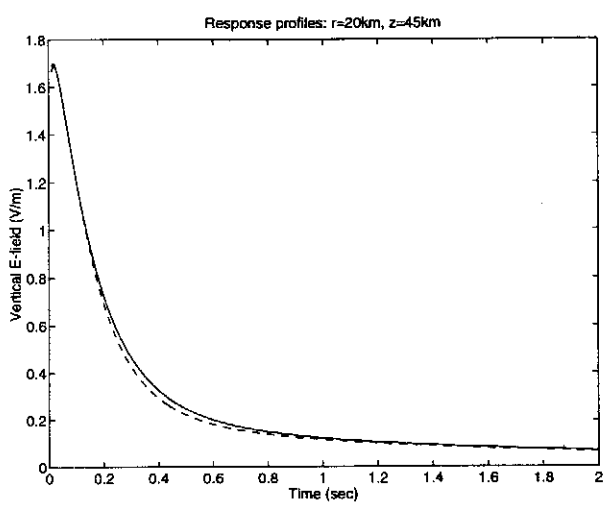

Figure 8: Electric field transient (altitude 45km)

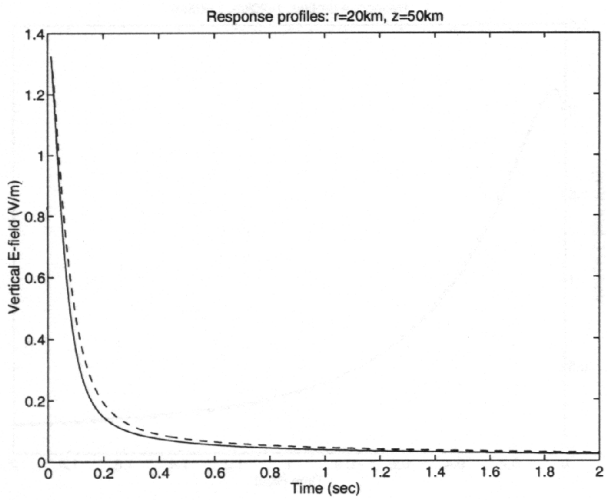

Figure 9: Electric field transient (altitude 50km)

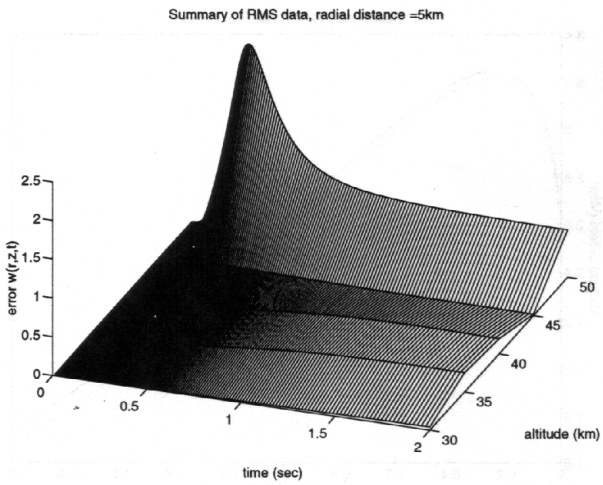

Figure 11: Error at radial distance 5km

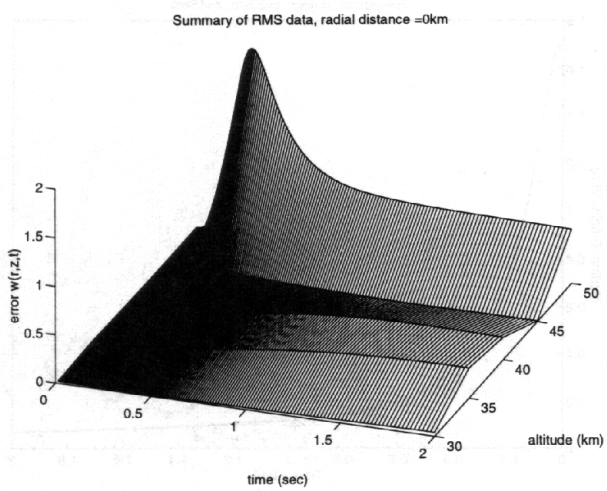

Figure 10: Error at radial distance 0km

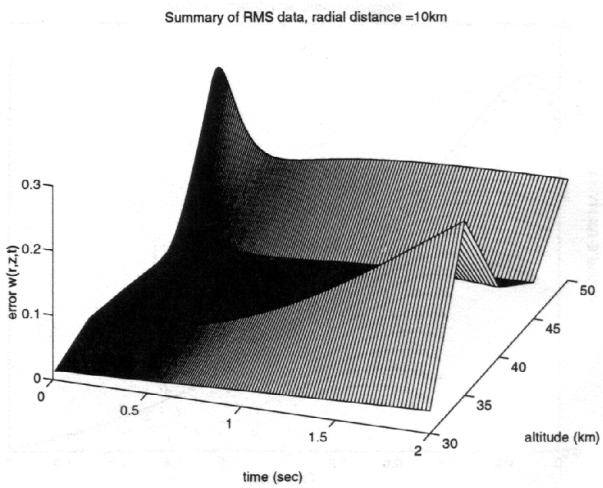

Figure 12: Error at radial distance 10km

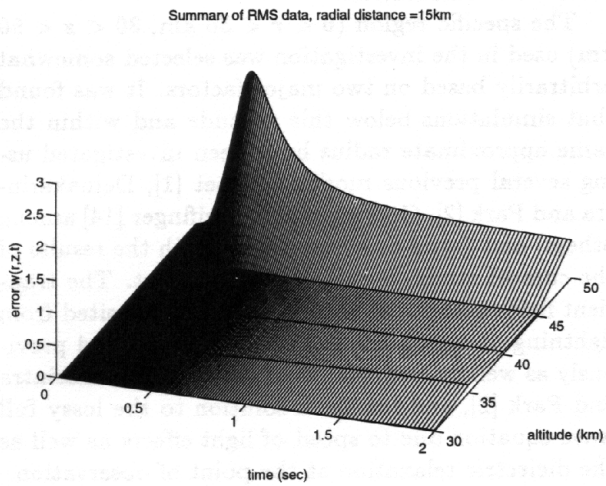

Figure 13: Error at radial distance 15km

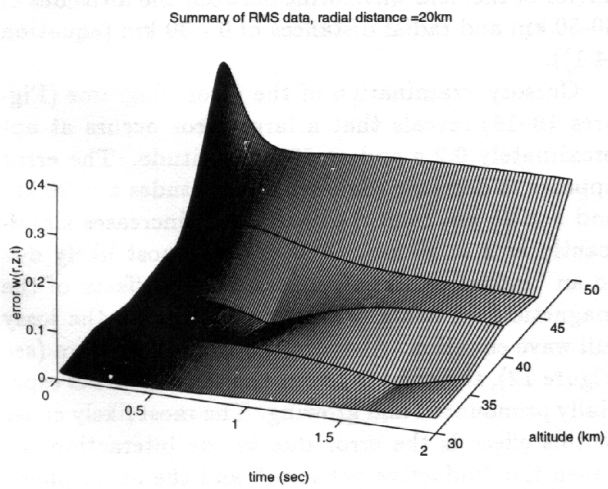

Figure 14: Error at radial distance 20km

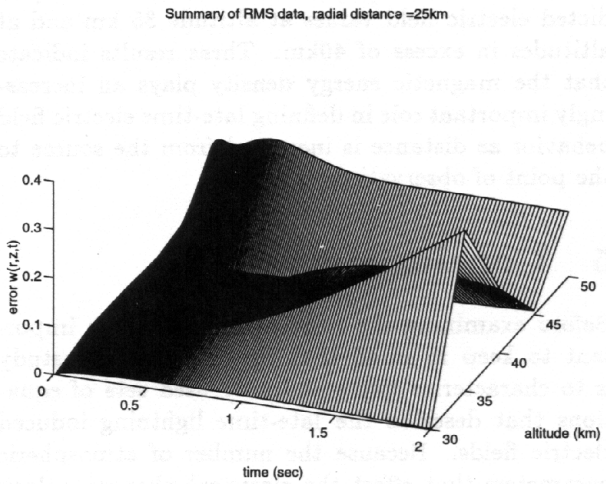

Figure 15: Error at radial distance 25km

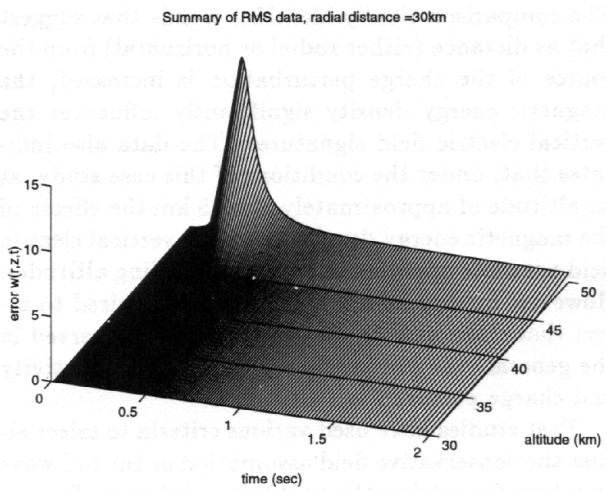

Figure 16: Error at radial distance 30km

Error comparisons were also made using de_∞/dt and de_c/dt; results were consistent with those of the electric field waveforms themselves. In each of these cases, a clear distinction can be seen between predicted electric field values at altitude 35 km and at altitudes in excess of 40km. These results indicate that the magnetic energy density plays an increasingly important role in defining late-time electric field behavior as distance is increased from the source to the point of observation.

5 Conclusions

Before examining the results in detail, it is important to keep in mind that the focus of this study is to characterize two standardly used sets of equations that describe the late-time lightning induced electric fields. Because the number of atmospheric parameters that effect the electrical phenomenology is large (e.g., ϵ, σ, scale height, cloud conductivity), this study serves as a precursor for future endeavors that can investigate the electric fields' sensitivity to all constitutive parameters as well as the effects that variable boundary conditions will have.

A comparison was made between the values of late-time the vertical electrical field magnitude predicted by (1) the continuity equation and Poisson's equation and by (2) the continuity equation in conjunction with the lossy wave equation, respectively. The comparison clearly identifies trends that suggest that as distance (either radial or horizontal) from the source of the charge perturbation is increased, the magnetic energy density significantly influences the vertical electric field signatures. The data also indicates that, under the conditions of this case study, at an altitude of approximately $z = 35$ km the effects of the magnetic energy density upon the vertical electric field are more apparent than at surrounding altitudes. However, further intensive studies are required to assert that these qualitative schema will be observed in the general case over arbitrary values of conductivity and charge perturbation altitudes.

Past studies have used various criteria to select either the conservative field assumption or the full wave equation for solving the problem of interest. For example, Dejnakarintra and Park [2] compare the conductivity σ to the susceptivity $j\omega\epsilon_0$ in order to decide which assumptions to use. Nisbet [1] implicitly advocates the use of a conservative field assumption since his model uses resistive and capacitive elements but not inductive elements. At present, the applicability of the conservative field assumption for late-time electric field recoveries resulting from lightning remains somewhat controversial.

The specific region ($0 < r < 30$ km, $30 < z < 50$ km) used in the investigation was selected somewhat arbitrarily based on two major factors. It was found that simulations below this altitude and within the same approximate radius have been investigated using several previous models (Nisbet [1], Dejnakarintra and Park [2], Greifinger and Greifinger [14] among others) and found to be consistent with the results of the current study, hence, of little interest. The transient fields associated with the charge deposited from lightning above 50 km have been investigated previously as well by Baginski *et al* [15] and Dejnakarintra and Park [2], and require a solution to the lossy full wave equation due to speed of light effects as well as the dielectric relaxation at the point of observation.

The investigation demonstrated that: 1) If the widely used conservative field assumption ($\nabla \times E = 0$) is rigorously enforced (both of Maxwell's curl equations solved simultaneously) then the electric field may only exhibit exponential decay that is generally in error. 2) When the two solutions of the late-time transient event (one using the conservative field assumption and omitting Faraday's Law of induction, the other solving the complete lossy wave equation) are compared, there is a measurable error in the behavior of the field waveforms between the altitudes of 30-50 km and radial distances of 0 - 30 km (equation (4.1)).

Cursory examination of the error diagrams (Figures 10–16) reveals that a large error occurs at approximately 0.2 s and at 50 km altitude. The error appears to decrease somewhat at altitudes $z = 20$ km and $z = 25$ km from the source, but increases significantly at $z = 30$ km. This error is most likely due to an "inductive surge" caused by the effects of the magnetic field being taken into account in the lossy full wave equation. At radial distance $r = 10$ km (see Figure 12), the error between the two models is especially pronounced and growing. The most likely cause of this effect is the error due to the interaction between the "inductive behavior" and the atmospheric time constant at the point of observation.

Acknowledgement The authors wish to thank Marcus Lankford for his assistance in preparation of the simulations in this study. The authors also wish to express their thanks to the reviewers for their many

helpful suggestions and improvements to the paper.

References

[1] John S. Nisbet. A dynamic model of thundercloud electric fields. *J. Atmos. Sciences*, 40:2855–2873, 1983.

[2] M. Dejnakarintra and C. G. Park. Lightning-induced electric fields in the ionosphere. *Journal of Geophysical Research*, 79(13):1903–1909, 1974.

[3] Michael E. Baginski. *Finite Element Simulation of the Atmosphere's Electromagnetic Response to Charge Perturbations Associated with Lightning.* PhD thesis, The Pennsylvania State University, 1987.

[4] C. E. Baum. Simulation of electromagnetic aspects of lightning. In *Proceedings of Lightning Technology, NASA Conference*, April 1980.

[5] R. H. Holzworth and Chiu Y. T. Chui. Spherics in the stratosphere. In *CRC Handbook of Atmospherics*, volume 1. CRC Press, Boca Raton, Florida, 1982.

[6] R E. Holzer and D. S. Saxon. Distribution of electrical conducting currents in the vicinity of thunderstorms. *Journal of Geophysical Research*, 57(207), 1952.

[7] M. A. Uman. *Lightning.* McGraw-Hill, New York, 1969.

[8] Y. A. Tamura. An analysis of the electric field after lightning discharges. *Geophys. Res. Paper*, 42:190–200, 1955.

[9] H. Kasmir. The thunderstorm as a generator in the global electric circuit. *Z. Geophys.*, 25:33, 1959.

[10] F. J. Anderson and G. D. Freier. Interaction of a thunderstorm with a conducting atmosphere. *J. Geophys. Res.,*, 74:5390, 1969.

[11] C. T. R. Wilson. Some thundercloud problems. *J. Franklin Inst.,*, 208, 1916.

[12] A. J. Illingworth. Electric field recovery after lightning as a response of a conducting atmosphere to a field change. *Quart. J. Roy. Meterorol. Soc.*, 98:604, 1972.

[13] C. G. Park and M. Dejnakarintra. Penetration of thundercloud electric fields into the ionosphere and magnetosphere 1. middle and subauroral latitudes. *Journal of Geophysical Research*, 78:6623–6633, 1973.

[14] C. Greifinger and P. J. Greifinger. Electric fields in the atmosphere. *Journal of Geophysical Research*, 81:2237–2247, 1976.

[15] M. E. Baginski, L. C. Hale, and J. J. Olivero. Lightning related fields in the ionosphere. *Geophysical Research Letters*, 15(8):764–767, August 1988.

[16] Keven T. Driscoll, Richard J. Blakeslee, and Michael E. Baginski. A modeling study of the time-averaged electric currents in the vicinity of isolated thunderstorms. *Journal of Geophysical Research*, 97(D11):11,535–11,551, July 20 1992.

[17] P. Ratnamahilan P. Hoole and S. Ratnajeevan H. Hoole. Finite element computation of magnetic fields from lightning return strokes. In Z. J. Cendes, editor, *Computational Electromagnetics*, pages 229–237. North Holland, July 1986.

[18] P. Ratnamahilan P. Hoole and S. Ratnajeevan H. Hoole. Guided waves along an unmagnetized lightning plasma channel. *IEEE Trans. Magn.*, MAG-24(8):3165–3167, November 1988.

[19] H. Israel. *Atmospheric Electricity*, volume two. Israel Program for Scientific Translations, Jerusalem, 1973.

[20] E. D. Sunde. *Earth Conduction Effects in Transmission Systems.* Dover, New York, 1968.

[21] J. A. Chalmers. *Atmospheric Electricity 2nd edition.,*. Pergamon New York, 1967.

[22] A. J. Illingworth. Charge separation in thunderstorms: small scale processes. *Journal of Geophysical Research*, 90:6026, 1985.

[23] H. Volland. *Quasi-Electrostatic Fields within the Atmosphere.* CRC Press, Boca Raton, Florida, 65, 1982.

[24] H. Volland. *Atmospheric Electrodynamics,Chemistry in Space.* Springer-Verlag, Berlin, Germany, 1984.

[25] J. A. Stratton. *Electromagnetic Theory.* McGraw Hill, New York, 1941.

[26] R. H. Golde. *Lightning, Volume I.* Academic Press, 1977.

[27] L. C. Hale. Middle atmosphere electrical structure, dynamics, and coupling,. *Adv. Space Res.*,, 4:175–186, 1984.

[28] R. Courant and D. Hilbert. *Methods of Mathematical Physics.* Interscience, New York, 1962.

[29] Karl S. Kunz and Raymond J. Luebbers. *The Finite Difference Time Domain Method for Electromagnetics.* CRC, 1993.

[30] Granville Sewell. *Analysis of a Finite Element Method: PDE/PROTRAN.* Springer-Verlag, 1985.

[31] Granville Sewell. *The Numerical Solution of Ordinary and Partial Differential Equations.* Academic Press, New York, 1988.